Available online at www.sciencedirect.com
SCIENCE DIRECT
Thin-Walled Structures 44 (2006) 692–700
THIN-WALLED STRUCTURES
www.elsevier.com/locate/tws

Crashworthiness assessment of square aluminum extrusions considering the damage evolution

J.S. Qiao*, J.H. Chen, H.Y. Che

College of Material Science and Technology, Lanzhou University of Technology (LUT), Lanzhou (730050), China

Received 23 December 2005; accepted 20 April 2006
Available online 10 July 2006

Abstract

Combining the pivotal tests and FEM technology, crashworthiness of aluminum extrusions was studied for an automobile safety plan. Experiments under static axial loading conditions were carried out for square thin-walled tubes with different thicknesses, section dimensions, with various impact velocities were conducted as well. Crush behavior of this structure under axial static and dynamic loads was studied. FEM code was used for crash analysis, which gave deformation and load prediction. Geometric imperfection and damage model were introduced to simulation. Results show that experiment and numerical model have good agreement with each other.

Keywords: Thin-walled aluminum extrusion; Crashworthiness; Inflectional distortion; FEM

1. Introduction

As a result of energy shortage and environmental problem in the world, automotive manufacturers should pay more attention to the new concept about lessen fuel consumption and lower carbon dioxide (CO_2) emissions. Light weight vehicle such as aluminum space-frame cars attract designer's eyeballs, because of that their weight savings of as much as 25% may be possible compared with conventional steel structures. What's more, aluminum alloy has good corrosion resistance and high capability of energy absorbing.

Aluminum extrusions are wildly used in energy-absorbing systems for automobile, due to that complicated cross-sections, these members show good performance on energy absorbing. When crash accident occurs, distortion such as bending, torsion and folding would be mainly concentrated to these sections and minimal acceleration is transferred to the occupants. So the crashworthiness of aluminum extrusions has great effect on the energy absorbing of absorber. A great amount of research has been carried out on this object. M. Langseth and O.S. Hopperstad have studied the behavior of aluminum extrusions under axial loading conditions in detail, and gave test data for validation of a numerical model in code LS-DYNA. Furthermore, they also studied the combined distortion of extrusions and aluminum foam filler [1–5,8]. Deb and Mahendrakumar presented a design of an aluminum-intensive vehicle platform for front impact safety, which addressed to the crashworthiness of a space frame structure with welded extrusions [6]. Their experimental observations on aluminum tubes with T joints show good agreement to the numerical simulation results which identified that the design approach of component-level testing combined with finite element and lumped parameter-based simulations could be an effective way in new vehicles safety evaluation.

Common to the work so far on the crashworthiness of aluminum extrusions, experimental results show that in front impact accident, girders and beams made of extrusions are mainly components for energy absorbing. Crashworthiness of aluminum extrusions is affected by material microstructure, loading speed and geometrical dimensions. In addition, the material damage evolution and deformation inconsonance should also be considered as well, which will lead more accurate simulation results, when a reasonable numerical model is established. In the following parts of this paper, a test program is represented to examine the folding process of aluminum extrusions. The experimental data would be combined with a

*Corresponding author. Tel.: +86 931 3936271; fax: +86 931 2806962.
E-mail address: qiaojisen@lut.cn (J.S. Qiao).

0263-8231/$ - see front matter © 2006 Elsevier Ltd. All rights reserved.
doi:10.1016/j.tws.2006.04.015

Table 1
Sample list

Test/simulation	Thickness	Length	Cross-section	Sample No.	Load condition	Static/impact velocity
Test data	1	100	76 × 25	1-L1-2S-T	S	St
				1-L1-1D-T	Q–S	1.4909
				1-L1-2D-T	Q–S	2.1112
				1-L1-3D-T	Q–S	2.2889
				1-L1-4D-T	Q–S	2.3185
				1-L1-5D-T	Q–S	2.3537
				1-L1-6D-T	Q–S	3.3339
	2	200	76 × 44	2-L2-1S-T	S	St
Numerical model	1	100	76 × 25	1-L1-1S-N	S	St
				1-L1-1D-N	Q–S	1.4909
				1-L1-2D-N	Q–S	2.1112
				1-L1-3D-N	Q–S	2.2889
				1-L1-4D-N	Q–S	2.3185
				1-L1-5D-N	Q–S	2.3537
				1-L1-6D-N	Q–S	3.3339
	2	200	76 × 44	2-L3-1S-N	S	St

numerical model considering the damage initiation and evolution as well as geometric imperfection.

2. Crash test

2.1. Test program and experimental setup

For aluminum extrusions subjected to axial loading, the reported experimental data as well as the experimental details are limited. Most of the published work is related to circular tubes and spot-weld-bonded box sections. Therefore, an extensive experimental research project has been carried out to study the behavior of thin-walled aluminum extrusions subjected to axial loading and to provide data for validation studies of computer codes.

The objective of this part of the research project was: (1) To study the static and dynamic behavior of square thin-walled tubes subjected to axial loading in conditions varying the wall thickness specimen, length, and impact velocity. (2) To study any difference in behavior between static and dynamic tests.

Two different wall thicknesses and lengths of extrusions were tested under dynamic and static axial loading conditions. Furthermore, large amount of numerical models have been carried out under different geometric and load conditions (Table 1). Among these models, some of them are of test validation. By comparing the computation results to the test data, it was sure that the simulation supplied good predication. Others were useful testing complements, which predict the in case crashing behavior of the square tubes. Fig. 1 shows the experiment boundary conditions: the square tube was placed on the worktable with a steel plate covering on the top. For static crashing, the crosshead of test machine would go down to compress the tube with a velocity of 1 mm/min; for quasi-static and dynamic loading, a drop hammer would impact the tube on the top with the muzzle velocities range from 0.6033 to 3.3339 m/s. since the buckle of thin walled extrusions is sensitive to the initiation structure. Prior to testing, thickness of the specimens was measured carefully and the error of average thickness of qualified specimens is less than 5% according to reference document [3].

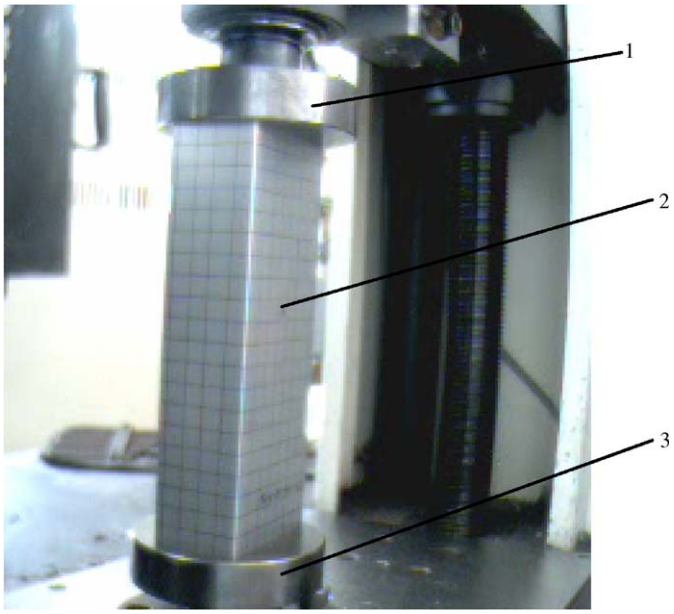

Fig. 1. Test device: (1) up plate, (2) extrusion and (3) support plate.

2.2. Material properties

Test specimens were made of the aluminum alloy 6063 tempers T6. Fig. 2 shows the typical engineering stress–stain curve for the material tested. After extrusion the profiles were air cooled and stretched to an elongation of 1–2%, Temper T6 means that the alloy was aged for 2 h at 195 °C.

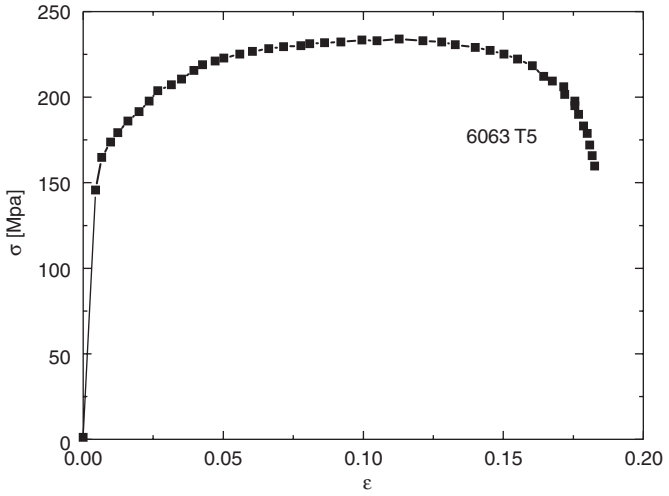

Fig. 2. Material engineering strain–stress curve.

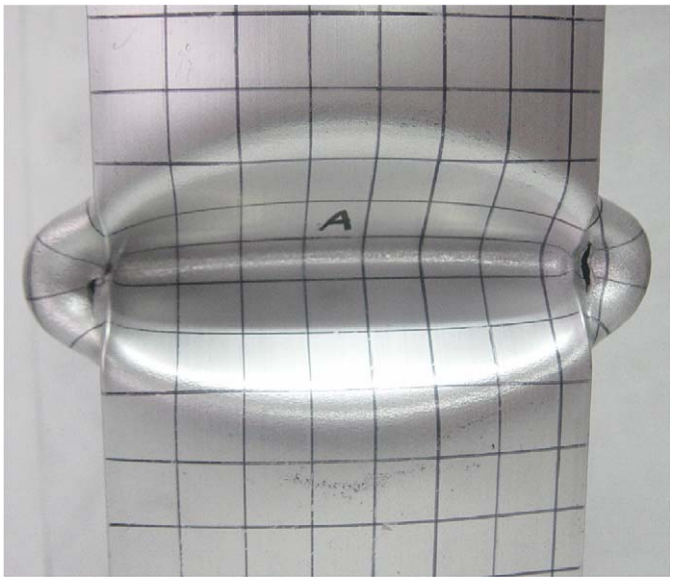

Fig. 3. Cracks taking place during crashing.

Based on the research results in literature [11–13], mechanical properties of aluminum alloy 6000 series is estimated to be nor sensitivity to the strain rate, the 0.2% proof stress and ultimate stress change little (within 5–10%) within the strain rate range from 10^{-4}–$10^{-3}\,s^{-1}$. So that we can use the material date obtained form the static tensile test for the dynamic test analysis and numerical modeling.

2.3. Test results and discussion

2.3.1. Visual observation

For the static compressing test, the sample was placed on the worktable with its top covering by a steel plate. The crosshead went down to compress the tube and the loading velocity was keeping constant of 1.0 mm/min. From repetitious testing, conclusion can be obtained that the unstable deformation always initiates on the two sidewalls, which the wider sides of the square cross section belong. The two wider side walls would be protruded or recessed by chance and then similar distortion would be triggered on the two other side walls, until a folding lobe was coming into being. If the plasticity of tube were good enough, this deformation would happen periodically, until the tube was completely crashed. But, in most case cracks took place during the crash process (see Fig. 3). Because the local deformation has reached the critical value, and thus the rupture took place in the area. When the crack came into being, the ability of energy absorbing was dropped down sharply for the tube, which means the energy absorber was damaged, and the load carrying capacity would go down quickly, distortion of the tube become uncertain (Fig. 4). Many tests have been done to study the folding and cracking. Some useful information has been gotten from these researches.

For the dynamic crashing test, the sample had the same boundary condition as that for the static test. A drop hammer went down to hit the tube with different initial impact velocity. Either symmetric or a combination of symmetric and asymmetric modes were observed for the thinner specimens. Furthermore, twist deformation and band collapse were observed compared with folding process (Fig. 5). Fracture was found in some of the short specimens, some crack located at the top of the tube, some at the body corners, the force and internal energy record curves of the impacted process show that for thin-walled extrusions under quasi-static loading these observed cracks have no influence on global response. But for thick-walled extrusions under static compressing, once the cracks occurred the folding process stopped, large tear distortion was observed in crack zone (Fig. 6). Following section would give more details about damage evaluation.

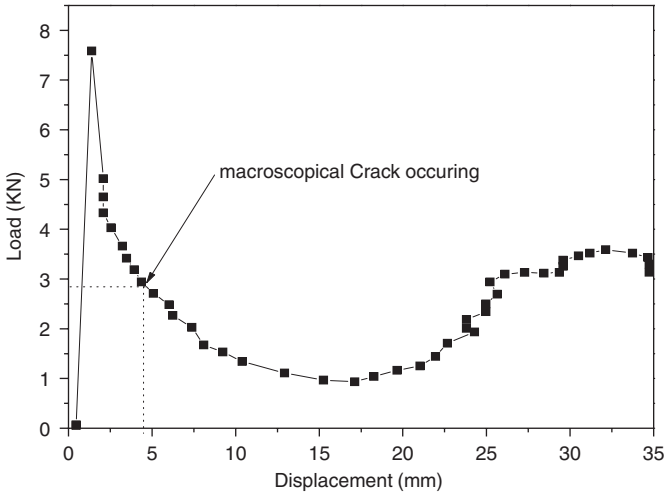

Fig. 4. Static load–displacement curve.

2.3.2. Effect of wall thickness on crash behavior

The wall thickness has little influence on the deformation shape, however, influences the measured force rounded by

Fig. 5. Twist and band deformation modes dynamic crashing for thin-walled extrusion.

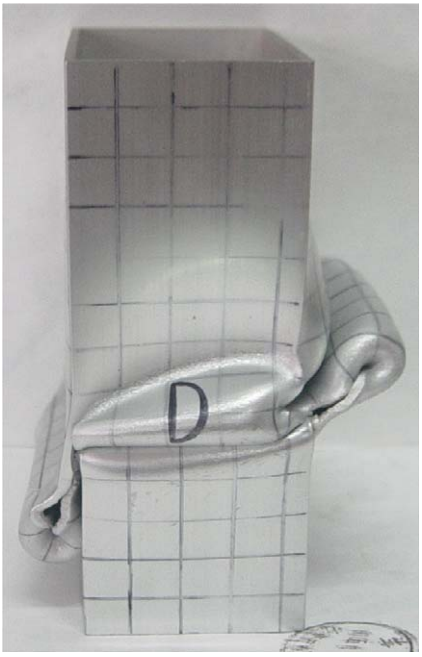

Fig. 6. Tear distortion in crack zone.

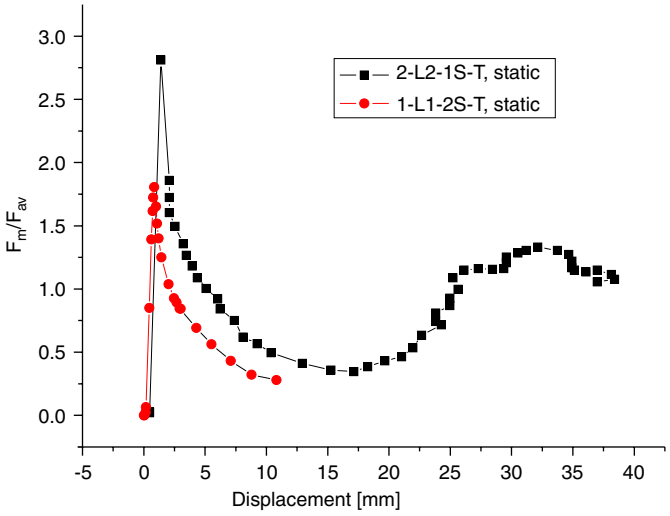

Fig. 7. Ratio between measured load and mean loads versus displacement. Effect of thickness.

average force level F_M/F_{av}. A thick wall increases F_M/F_{av} compared to that of a thin wall, see Fig. 7.

Fig. 8 also shows that E_{MI} (measured absorbed energy) is much higher for an extrusion with thicker wall than that for a thinner extrusion.

2.3.3. *Effect of impact velocity on crash behavior*

Figs. 9 and 10 show that both peak load and impact energy increased with the impact velocity. As the strain rate assumed to have little influence on mechanical properties, the observed increasing has to be associated with inertia effects set up at the instant of impact in the folding process.

3. Numerical modeling

In the following sections, a numerical modeling about axially loaded square aluminum extrusion of alloy 6063 T6 are presented. The simulation are carried out with the computer code ABAQUS standard and explicit. Results from these non-linear finite element modeling are compared with the present test data given in Section 2. Our main objective is to confirm the validity and accuracy of the theoretical predictions, which includes the assumptions about the geometry imperfection and damage evolution.

3.1. *Numerical modeling of static and dynamic test*

As both symmetric and a combination of symmetric and asymmetric modes were observed during deformation, specimens were modeled using their complete dimensions,

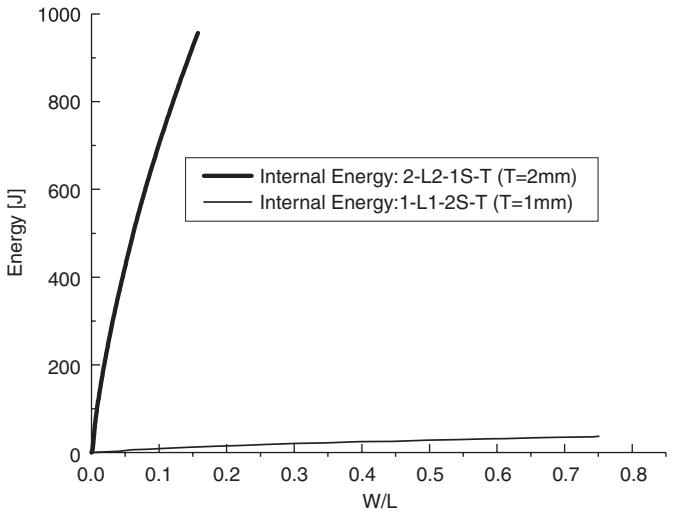

Fig. 8. Energy versus relative deformation: W—displacement, L—total length.

and the S4R shell element was selected to mesh the extrusions. The crosshead and drop hammer were modeled using two symmetry planes meshed with rigid shell element R3D4. The contact between the plate and square tube was modeled using a surface-to-surface contact pair with friction coefficient of 0.3. The contact between the lobes during deformation was modeled using double surface self-contact algorithm with friction coefficient of 0.15 in order to study the influence of friction on interaction of two contact surfaces, another numerical model was set up with frictionless for the contact pairs.

There are many buckle modes for extrusion deformation when the square tubes are compressed axially. These buckle modes will work together to cause the initial imperfections during pro-folding process and make significant effect on the crush behavior of extrusion in the followed folding process. But not all the modes have same weight coefficient, actually for static and quasi-static the two low-amplitude modes have the

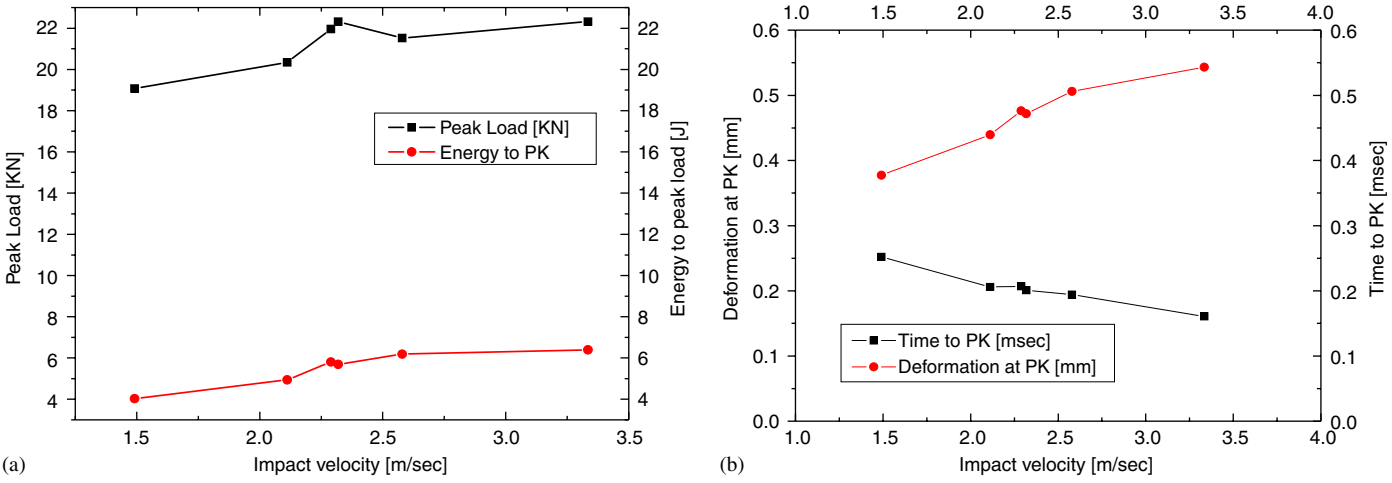

Fig. 9. Effect of impact velocity: (a) peak load and the energy to peak load versus impact velocity and (b) deformation and time to peak load versus impact velocity.

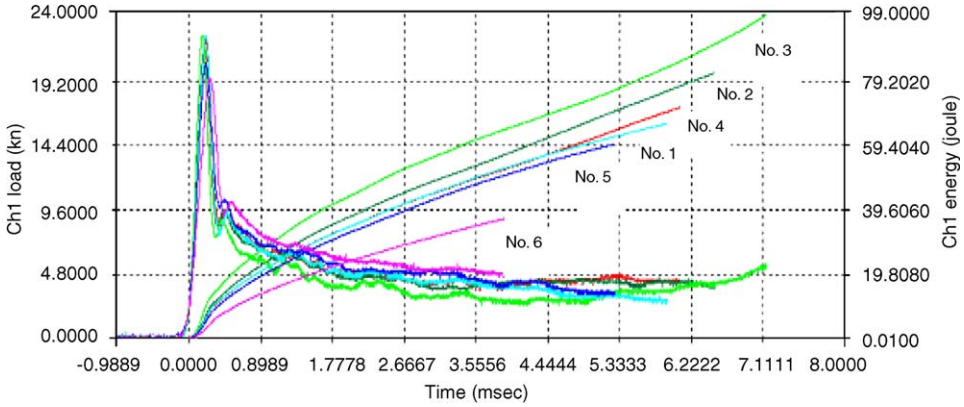

Fig. 10. Force displacement/energy time curves for drop hammer test No. 1: $V = 2.2889\,\mathrm{m/s}$; No. 2: $V = 2.5786\,\mathrm{m/s}$; No. 3: $V = 3.3339\,\mathrm{m/s}$; No. 4: $V = 2.3185$ No. 5: $V = 2.1112\,\mathrm{m/s}$; No. 6: $V = 1.4909\,\mathrm{m/s}$.

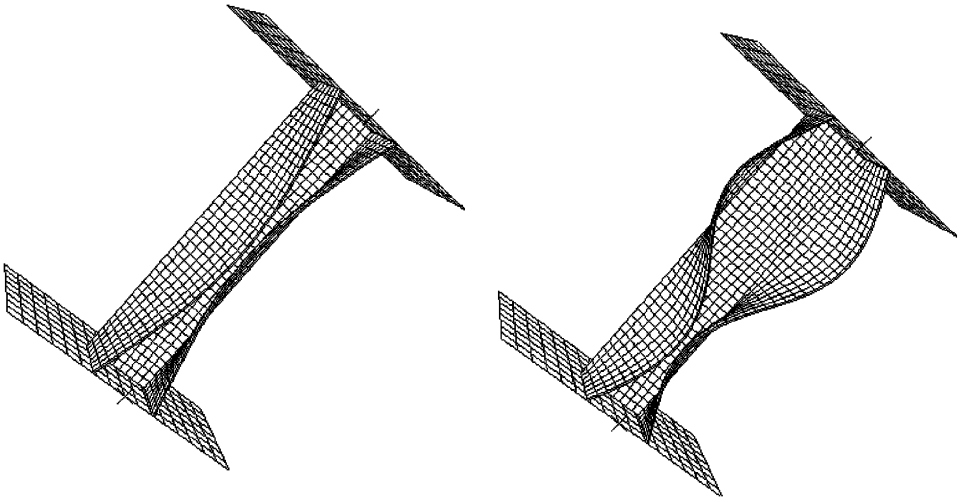

Fig. 11. Low-frequency buckle modes.

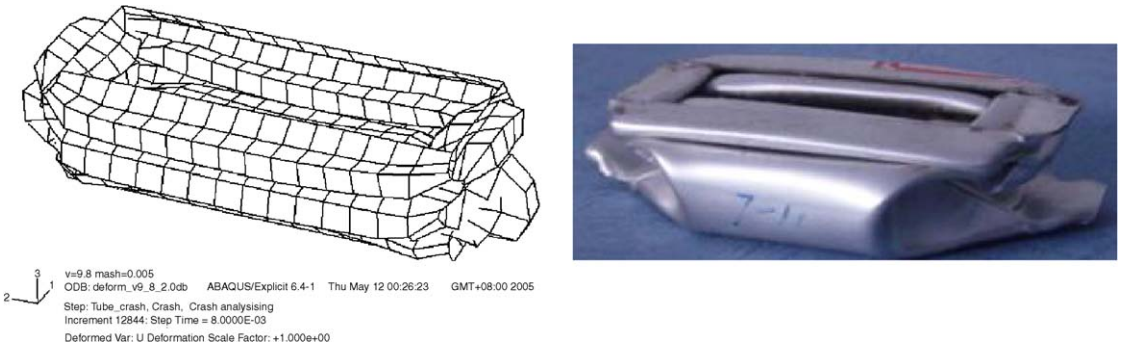

Fig. 12. Deformation comparison between test and simulation $V = 1.4909\,\mathrm{m/s}$.

dominant influence on crush behavior, (Fig. 11), the others do little effect, which can be ignored. Only in high-speed impact simulation, these high-amplitude modes should be considered.

According to this assumption, we calculated 10 modes for each numerical model using ABAQUS STANDARD code. For static or quasi-static loading case, modes 1 and 2 were introduced in crush simulation as geometric imperfection. For dynamic loading case, all 10 modes were combined by pulsing their weight coefficient as integral imperfection trigger. Results show that these asymmetric high-amplitude modes will cause twist or collapse distortion during crashing, which have good agreement with the test data in document [3].

In the present analyses, a material model is established as follows: the aluminum alloy is modeled as an elastroplastic material, using isotropic elasticity, von Mises yield criterion and an associated flow rule. The σ–ε curve was obtained by digital transacting of Fig. 2. Strain rate effects were not included as the material was assumed to be almost strain rate insensitive.

A shear failure damage model was used to describe the crack initiation and evolution [14–16]. The shear criterion is a phenomenological model for predicting the onset of damage due to shear band localization. The model assumes that the equivalent plastic strain at the onset of damage $\bar{\varepsilon}_s^{pl}$, is a function of the shear stress ratio and strain rate: $\bar{\varepsilon}_s^{pl}(\theta_s, \dot{\bar{\varepsilon}}^{pl})$.

Here $\theta_s = (q + k_s p)/\tau_{\max}$ is the shear stress ratio, p is the pressure stress, q is the Mises equivalent stress, $\tau_{\max}$ the maximum shear stress, and k_s is a material parameter. The criterion for damage initiation is met when the following condition is satisfied:

$$\omega_S = \int \frac{\mathrm{d}\bar{\varepsilon}^{pl}}{\bar{\varepsilon}_S^{pl}(\theta_s, \dot{\bar{\varepsilon}}^{pl})} = 1,$$

where ω_S is a state variable that increases monotonically with plastic deformation proportional to the incremental change in equivalent plastic strain.

Once the damage initiation criterion has been reached, the damage evolution started, the effective plastic displacement $\bar{u}^{pl}$, is defined with the evolution equation

$$\dot{\bar{u}}^{pl} = L\dot{\bar{\varepsilon}}^{pl},$$

where L is the characteristic length of the element.

We assume the evolution of damage is in the form of linear with effective plastic displacement; the damage

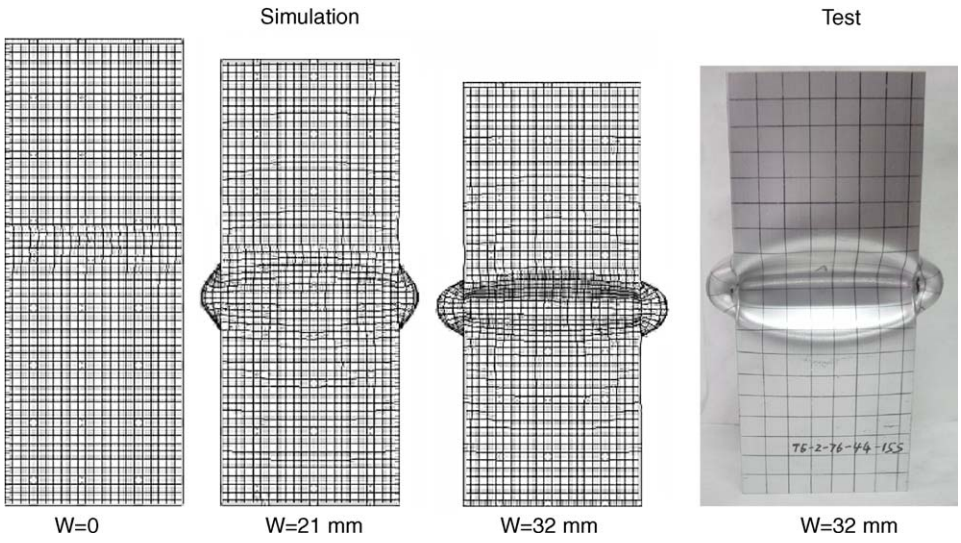

Fig. 13. Static analysis, deformation modes for sample 2-L2-1S-T.

variable can be identified as

$$\dot{d} = \frac{L\dot{\bar{\varepsilon}}^{pl}}{\bar{u}_f^{pl}} = \frac{\dot{\bar{u}}^{pl}}{\bar{u}_f^{pl}}.$$

This definition ensures that when the effective plastic displacement reaches the value $\bar{u}^{pl} = \bar{u}_f^{pl}$, the material stiffness will be fully degraded ($d = 1$). The linear damage evolution law defines a truly linear stress–strain-softening response only if the effective response of the material is perfectly plastic (constant yield stress) after damage initiation.

Based on the theory above, we added the following code lines to the ABAQUS EXPLICIT input file.

*DAMAGE INITIATION, CRITERION = SHEAR, $KS = 0$, 0.155.

*DAMAGE EVOLUTION, TYPE = DISPLACEMENT, SOFTENING = LINEAR 0.000075.

3.2. Validation

Figs. 12 and 13 show representative comparison of deformed specimen configuration between the test and numerical model for dynamic and static crush. As can be seen the final shape of test folding is well predicted by the numerical model, which means the simulation has remarkable value. In addition, it can be seen from Fig. 14 that the numerical model with geometric imperfection and damage evolution gives more accurate prediction of static crush comparing to other numerical models without damage evolution. Once the cracks occurred, the simulated load curve went down quickly, because of the material degeneration, which has been identified by the test.

Fig. 15 gives the detail information about crack evolution. In numerical model, crack occurred at the corner of extrusion, and spread along the edge, this process has good agreement with test observation.

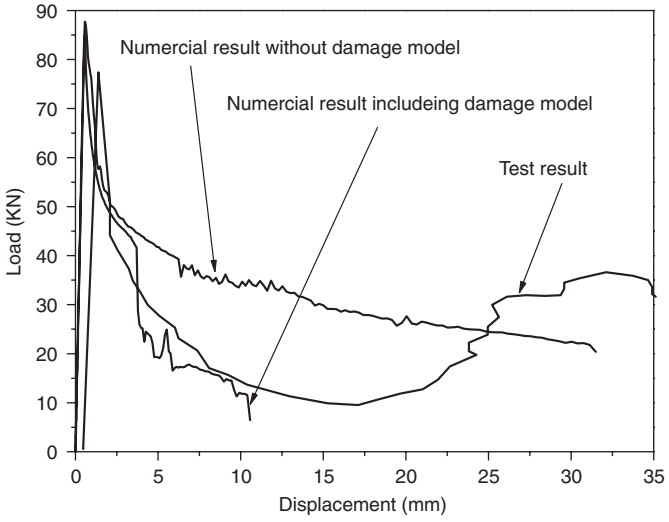

Fig. 14. Force–displacement curves comparison between simulation and experiment results.

Fig. 16 shows representative comparison between the simulated and experimental force–time curves for different samples under dynamic crush. The peak loads and shape of the simulated curves shows good agreement with these experimental ones. However, there is trend that during the post-buckling the numerical analysis over-predicts the load response, this maybe result from that we used idea discrete shell elements to represent the consecutive metal fibers, which would lead to a over-predict deformation resistance than actual samples. In addition observed during dynamic test, the recorder filter get rid of these high-frequency content due to elastic stress waves, which maybe cause some useful data got lost.

Mesh size is another factor, which has important influence on simulation accuracy. Mesh size makes great effect on the deformation modes and the peak load amplitude. As showed in Fig. 17 for this special extrusion

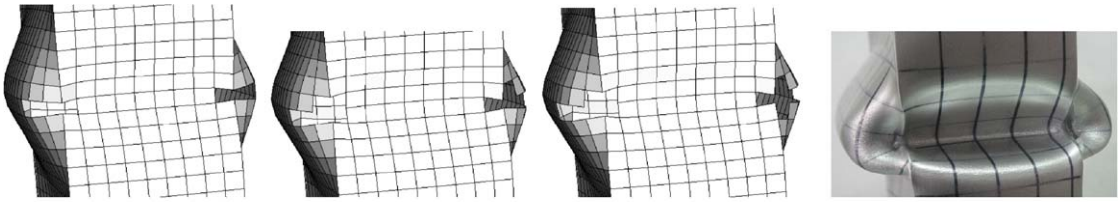

Fig. 15. Damage mode for crack initiation and evolution: (a) numerical mode for crack initiation and evolution and (b) crack taking place at first folding lobe. Test sample: 2-L2-1S-T, Displacement: 12 mm.

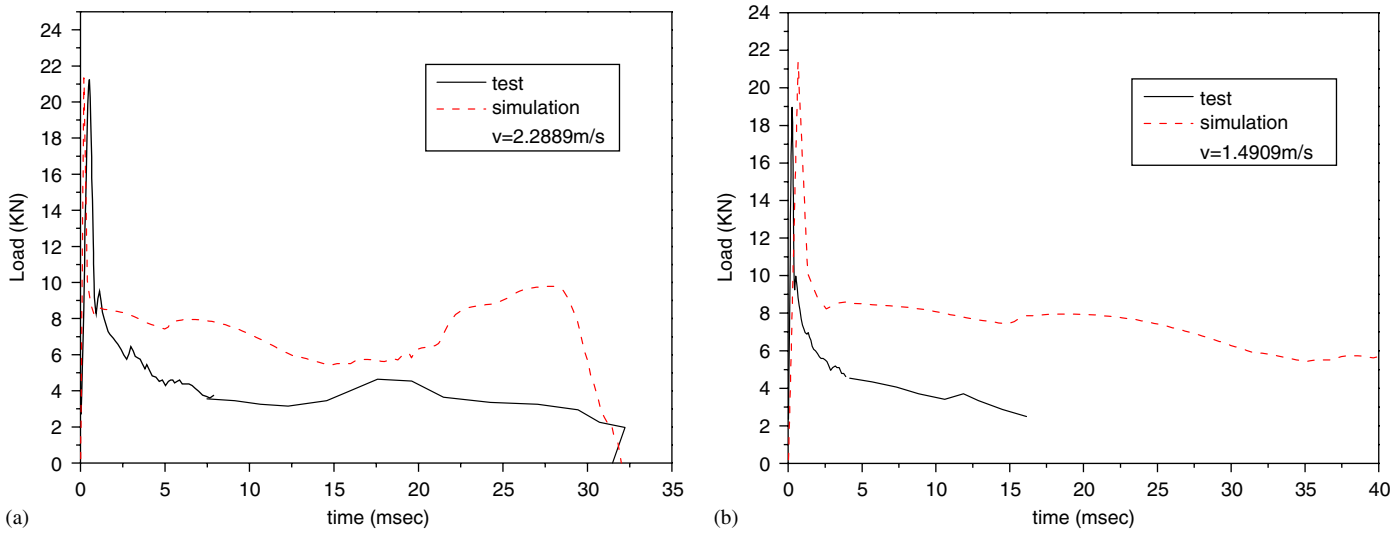

Fig. 16. Dynamic analysis comparison between test and numerical mode: (a) impact velocity: 2.2889 m/s and (b) impact velocity: 1.4909 m/s.

samples, reasonable mesh size is about 5 mm, which gives smooth analysis and good prediction of crush process both for deformation modes and load capacity prediction. Increasing or decreasing element size would lead the numerical result drift from test data as showed in Fig. 17. So how to decide a suitable mesh size is still a problem, which needs to be study deeply in the feature work.

Contact condition also needs to be thought over for numerical simulation. Two different contact conditions marked (a) and (b) were founded to describe the interaction. For condition (a), three contact pairs were founded. Interactions between two rigid plates and the extrusion were described as surface to surface contact pairs with friction coefficient of 0.3, self-contact property was assigned to the extrusion for self-interaction of the extrusion during folding with friction coefficient as 0.1; for condition b, the interactions between plates and extrusion were treated as frictionless behavior as well as the self-contact of extrusion.

These two different contact conditions caused different deformation modes as showed in Fig. 18. For case a, the localization of lobes started at the mid of extrusion; for case b the folding always occurred at the support end. However the peak load of two models are almost same (Fig. 19).

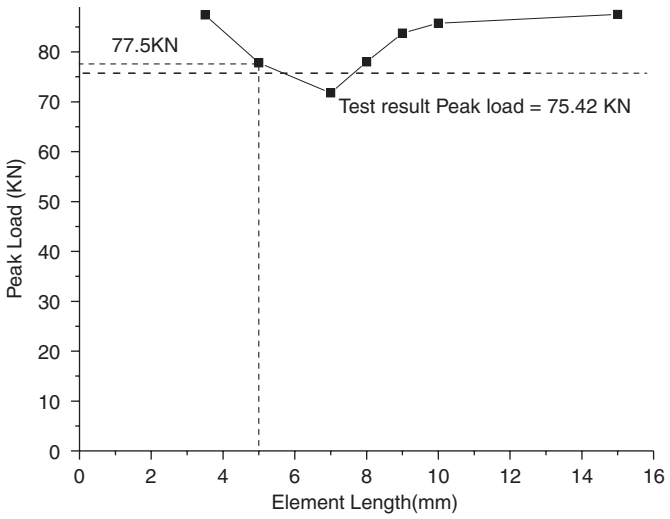

Fig. 17. Effect of mesh size on max load for static analysis Sample No: 2-L3-1S-N.

General speaking, for this specific extrusion samples, a reasonable numerical model with mesh size about 5 mm and contact condition of friction gives smooth analysis and good prediction of crush process

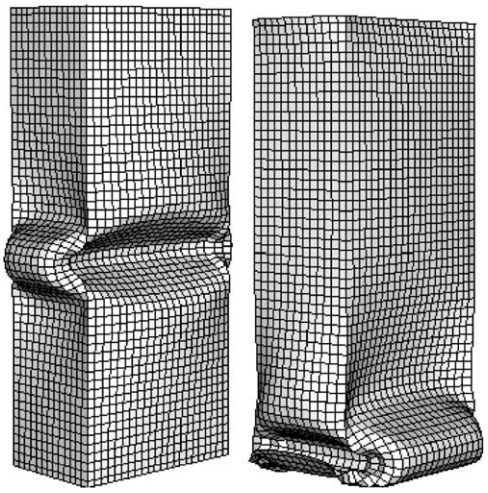

Fig. 18. Comparison of deformation modes. Effect of contact condition.

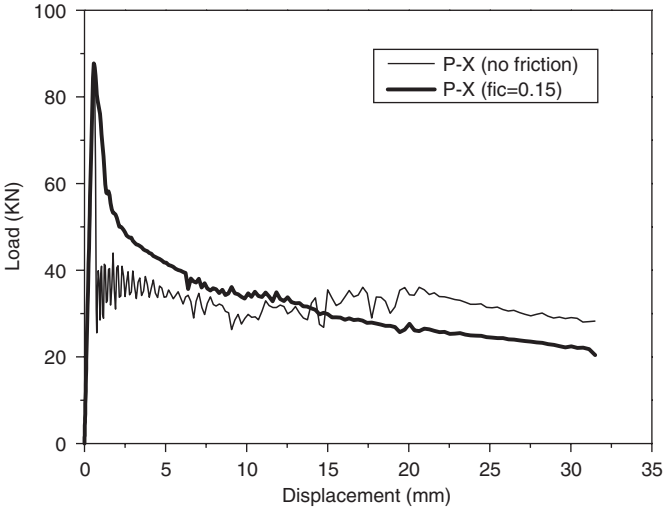

Fig. 19. Comparison between friction and frictionless load displacement curves.

4. Conclusion

Combining the pivotal tests and FEM technology, crashworthiness of 6063 AL alloy square tube under axial loading was studied for Automobile safety plan. Results show that crashworthiness of aluminum alloy tube is affected by material microstructure, impact speed, boundary conditions and geometrical dimensions. The most important findings from our research by now are proposed as follows:

(1) impact velocity makes great effect on load response and deformation modes. Peak load and impact energy increased with the impact velocity. For the high velocity, deformation modes change from symmetric to asymmetric or extensional collapse modes.
(2) the wall thickness has little influence on the deformation shape. However, effect the load capability greatly, as the mass specific average force F_{SM} can be improved by increasing the wall thickness.
(3) for the short-thin-walled extrusions ($L = 100$, $\delta = 1$ mm), the fracture seems have little effect on the global response. So the numerical mode can be set up without damage consideration. This because only one lobe comes into being during folding process, in this way contact condition seems more important for the numerical model. For the long thick wall extrusions ($L = 200$, $\delta = 2$ mm), damage model must be introduced to the simulation. Because the crack would lead the symmetric deformation modes to an unstable tear collapse failure. In addition that, the energy absorbing and carrying capacity are reduced obviously by the damage evolution. Results show that shear damage initiation criterion and linear softening damage evolution are suitable for the numerical model, which gives good prediction of crush process.
(4) geometric imperfection should be introduced to the simulation by combining the buckle modes to the crush analysis. Low-frequency modes have the dominant influence on crush behavior. High-frequency modes will cause twist or collapse distortion for dynamic analysis.
(5) mesh size and contact condition are another two influence factors to numerical model. For the comparison between test and simulation, as can be seen a reasonable element size is about 5 mm, friction must be thought over for contact surfaces.

References

[1] A Global perspective for tailored blanks laser welding. Canada: AWS Ltd.; 2000 January.
[2] Song HW, Wan Z, Xie Z, et al. Axial impact behavior and energy absorption efficiency of composite wrapped metal tubes [J]. Int J Impact Eng 2000;24:385–401.
[3] Langseth M, Hopperstad OS. Crash behaviour of thin-walled aluminum members [J]. Thin-Walled Struct 1998;32:127–50.
[4] Hanssen AG, Langseth M, Hopperstad OS. Static and dynamic crushing of square aluminum extrusions with aluminum foam filler [J]. Int J Impact Eng 2000;24:347–83.
[5] Andrews KRF, England GL, Ghani E. Classification of the axial collapse of cylindrical tubes under quasi-static loading [J]. Int J Mech Sci 1983;25(9–10):87–96.
[6] Deb A, Mahendrakumar MS. Design of an aluminium-based vehicle platform for front impact safety. Int J Impact Eng 2004;30:1055–79.
[8] Langseth M, Hopperstad OS. Local buckling of square thin-walled aluminium extrusions. Thin-Walled Struct 1997;27(1):117–26.
[11] Hanssen AG, Langseth M. Development in aluminium based crash absorption components. Norwegian–French Industrial Conference, Paris, November, 1996.
[12] Santosa S, Wierzbicki T. Crash behavior of box column filled with aluminium honeycomb or foam. Comput Struct 1998;68(4):343–67.
[13] Rodney JC. Response of material under dynamic loading. Int J Solid Struct 2000;37(3):105–13.
[14] ABAQUS analysis user manual. ABAQUS. Inc.; 2004.
[15] Hillerborg A, Modeer M, Petersson PE. Analysis of crack formation and crack growth in concrete by means of fracture mechanics and finite elements. Cement Concrete Res 1976;6:773–82.
[16] Oden JT, Pires EB. Nonlocal and nonlinear friction laws and variational principles for contact problems in elasticity. J Appl Mech 1983;50:67–73.